JOURNAL OF Materials CHEMISTRY

Local Er(III) environment in luminescent titanosilicates prepared from microporous precursors†

José P. Rainho,[a,b] Martyn Pillinger,[a] Luís D. Carlos,[b] Sidney J. L. Ribeiro,[c] Rui M. Almeida[d] and João Rocha*[a]

[a]*Department of Chemistry, University of Aveiro, 3810-193 Aveiro, Portugal. E-mail: ROCHA@DQ.UA.PT; Fax: +351 234 370084; Tel: +351 234 370730*
[b]*Department of Physics, University of Aveiro, 3810-193 Aveiro, Portugal*
[c]*Instituto de Química/UNESP, C. P. 355 CEP, 14800-900 Araraquara, Brasil*
[d]*Departamento de Engenharia de Materiais/INESC ID, Instituto Superior Técnico, Av. Rovisco Pais, Lisboa 1000-049, Portugal*

Received 6th August 2001, Accepted 11th January 2002
First published as an Advance Article on the web 21st February 2002

The local environment of Er^{3+} ions in microporous titanosilicate ETS-10 and in synthetic narsarsukite and glassy materials obtained by calcination of ETS-10 has been investigated by EXAFS, Raman and photoluminescence spectroscopies. Er L_{III}-edge EXAFS studies of Er^{3+}-doped ETS-10 support the view that the exchanged Er^{3+} ions reside close to the (negatively charged) TiO_6 octahedra. In ETS-10, Er^{3+} is partially bonded to framework oxygen atoms and hydration water molecules. The Er···Ti distance (3.3 Å) is similar to the Na···Ti distances (3.15–3.20 Å) reported previously for Na–ETS-10. Although the exact location of the ErO_6 units within the host structure of Er^{3+}-doped synthetic narsarsukite is still an open question, it is most likely that Er^{3+} substitutes Ti^{4+} rather than Na^+ ions. EXAFS spectroscopy indicates that no significant clustering of erbium atoms occurs in the titanosilicate samples studied. Evidence for the insertion of Er^{3+} ions in the framework of narsarsukite has been obtained by Raman spectroscopy. This is indicated by the increasing full-width at half-maximum (FWHM) of the 775 cm^{-1} peak and the increasing intensity of the anatase peaks as the erbium content increases. In addition, as the narsarsukite Er^{3+} content increases a band at *ca.* 515 cm^{-1} firstly broadens and subsequently a new peak appears at *ca.* 507 cm^{-1}. Er^{3+}-doped narsarsukite exhibits a characteristic local vibrational frequency, $\hbar\omega$ *ca.* 330 cm^{-1}, with an electron–phonon coupling, g *ca.* 0.2, which constitutes additional evidence for framework Er^{3+} insertion. The number of lines in the infrared emission spectrum of synthetic narsarsukite indicates the presence of two optically-active erbium centres with very similar local environments and an average $^4I_{13/2}$ lifetime of 7.8 ± 0.2 ms.

Introduction

Erbium-doped materials have attracted considerable attention in past years due to their potential applications in optoelectronics and telecommunications, essentially due to the intra-$4f^{11}$ transition between the first excited level ($^4I_{13/2}$) and the ground state ($^4I_{15/2}$) that occurs at *ca.*1.54 μm.[1–3] This wavelength corresponds to the window of minimum attenuation in the silica-based optical fibres currently used in optical communications.[1]

Recently, we have embarked on a comprehensive study aimed at evaluating the potential use of microporous solids as luminescent materials or as precursors for the preparation of materials for applications in optoelectronics. ETS-10, $[(Na,K)_2TiSi_5O_{13}\cdot xH_2O]$, is a large-pore titanosilicate material and one of the most important mixed octahedral/tetrahedral framework microporous solids.[4,5] The ETS-10 pore structure consists of 12-, 7-, 5-, and 3-rings and has a three-dimensional large-pore channel system whose minimum diameter is defined by 12-ring apertures. The disorder in ETS-10 arises from structural faulting along planes parallel to the 12-ring channel directions, and it is possible to describe the structure in terms of an intergrowth of two ordered polymorphs with tetragonal and monoclinic symmetry. Since ETS-10 contains corner-sharing TiO_6 octahedra and corner-sharing SiO_4 tetrahedra, for every framework titanium there is an associated −2 charge. This charge is compensated by extra-framework cations, usually Na^+ and K^+. Upon calcination in air at temperatures in the range of 1023–1173 K ETS-10 transforms into synthetic narsarsukite $[(Na,K)_2TiSi_4O_{11}]$, a dense tetragonal titanosilicate mineral made up of Si_4O_{10} chains which form tubes of rings of four SiO_4 tetrahedra.[6] These tubes are linked by chains of corner-sharing TiO_6 octahedra. The cavities between the Si_4O_{10} tubes and octahedral chains contain only Na^+ in the mineral narsarsukite and both Na^+ and K^+ ions in the synthetic material.

We have previously reported a method for the preparation of luminescent materials from precursor ETS-10 doped with Er^{3+} and Eu^{3+}.[7,8] Briefly, in this method Er^{3+} ions are introduced into the pores of ETS-10 *via* conventional ion-exchange techniques. The resultant material is subsequently calcined in air at temperatures in excess of *ca.* 973 K and it undergoes a phase transformation to synthetic narsarsukite. In the process, the Er^{3+} ions are trapped in the narsarsukite lattice. At *ca.* 1185 K synthetic narsarsukite melts and on cooling down an amorphous phase is obtained. Titanosilicate glasses are obtained at *ca.* 1473 K. Apart from the interesting photoluminescence features of these new lanthanide-doped titanosilicates,[7,8] very little is known about the local structure around the optically active ions. A precise evaluation of their potential for applications in optoelectronics and telecommunications requires knowledge of the local structure around the lanthanide

†Electronic supplementary information (ESI) available: Er L_{III}-edge k^3-weighted EXAFS spectra and Fourier transforms. See http://www.rsc.org/suppdata/jm/b1/b107136j/

 DOI: 10.1039/b107136j

This journal is © The Royal Society of Chemistry 2002

ions, which essentially determines the photoluminescence features. Extended X-ray absorption fine structure (EXAFS) spectroscopy yields information on the local surroundings of a chemical element, particularly the number and type of neighbours, interatomic distances and structural disorder and, thus, is a powerful tool for characterizing local environments.[9]

The aim of the present work is to study in detail the local environment of Er^{3+} ions in microporous titanosilicate ETS-10 and in materials obtained by calcination of this solid using EXAFS, Raman and photoluminescence spectroscopies. For Er^{3+}-doped titanosilicates this analysis, to our knowledge, has not yet been done. Even for other classes of materials modified by lanthanide salts only a limited number of studies, combining EXAFS and photoluminescence spectroscopies, is available on the local cation coordination.[10–15] In particular, here Er^{3+}-doped synthetic narsarsukite is examined in detail by excitation and Raman spectroscopy. This study complements the ^{29}Si MAS NMR and powder XRD work previously reported.[7] Phonon sideband spectra and the calculated phonon energy associated with a local Er^{3+} vibrational frequency as well as the electron-phonon coupling parameter, g, are determined for Er^{3+}-doped ETS-10 calcined at 973, 1073 and 1473 K.

Experimental

Sample preparation

The synthesis of ETS-10 has been previously described.[4] The experimental details of the method of preparation of luminescent titanosilicates can be found elsewhere.[7] The Er^{3+}-doped titanosilicates used in this study have a Ti/Er molar ratio of *ca.* 9, 11 and 23 (as ascertained by bulk, ICP-AES, chemical analysis). Er^{3+}-doped ETS-10 samples were calcined between 973 and 1473 K.

Techniques

Er L_{III}-edge EXAFS measurements were performed on station BM29 at the European Synchrotron Radiation Facility (ESRF), Grenoble, operating at 6 GeV in 2/3 filling mode with typical currents of 170–200 mA. The order-sorting double Si(311) crystal monochromator was detuned to give 50% harmonic rejection. The data were collected at room temperature and/or 50 K (Oxford cryostat) in transmission mode using ionisation chamber detectors. Each data point was collected for 3 s and in certain cases two scans were averaged. Samples were finely ground, diluted with BN, and formed into pellets. A reference sample of bulk Er_2O_3 was used as a model standard for determining co-ordination numbers and inter-atomic distances. The programs EXCALIB and EXBACK (SRS Daresbury Laboratory, UK) were used in the usual manner for calibration, summing and background subtraction of the raw data. EXAFS curve-fitting analyses, by least-squares refinement of the non-Fourier filtered k^3-weighted EXAFS data, were carried out using the program EXCURVE (version EXCURV98[16]) using fast curved wave theory.[17] Phase shifts were obtained within this program using *ab initio* calculations based on the Hedin Lundqvist–von Barth scheme. EXAFS data were analysed over the range Δk = 2.5–8.8 $Å^{-1}$ for the samples with the lower erbium loading and Δk = 2.5–10.5 $Å^{-1}$ for the samples with the higher erbium loading. All backscattering shells detailed in this article were found to have a probability of being insignificant of less than 1% according to the statistical test of Joyner *et al.*[18] The goodness of fit R-factor is defined as $R = \Sigma_i 1/\sigma_i(|\chi_i^{exp}(k) - \chi_i^{th}(k)|) \times 100\%$ and the fit index as $FI = \Sigma_i 1/\sigma_i\,[\mathrm{Exp}(i) - \mathrm{Theory}(i)]^2$, where $1/\sigma_i = k(i)^n/[\Sigma_j\ k(j)^n|\mathrm{Exp}(j)|]$. The program SEXIE[19] was used to calculate co-ordination shells and geometries for Er_2O_3, Na–ETS-10[20] and narsarsukite.[21] The model used in fit A only takes into account the erbium–oxygen shell, while in fit B one more shell of an element X is included.

Infrared emission spectra recorded in the temperature range 4.2–300 K were obtained on a Bruker IFS 66v Fourier transform infrared spectrometer (FTIR). The 488 nm line of an Ar ion-laser was used as the excitation source.

The frequency-domain lifetime measurements for the Er^{3+} $^4I_{13/2}$ excited level were performed at room temperature. A continuous Ar ion-laser (514.5 nm line) modulated by a chopper was used as the excitation source. A lock-in amplifier was used in the detection. The phase-angle shift (Φ) between the excitation (reference) and emission was measured as a function of the chopper frequency. The slope of the linear relation between the tangent of the phase-angle shift and the modulated frequency determines the emission lifetime.[22]

Unpolarized Raman spectra were measured with a Bruker RFS 100 FT-Raman Spectrometer in a backscattering geometry at room temperature with 2 cm^{-1} resolution, using a Nd–YAG laser for excitation, at 1064 nm, with approximately 100 mW power at the sample.

Results and discussion

EXAFS spectroscopy

The Er L_{III}-edge EXAFS of Er^{3+}-doped ETS-10 (Ti/Er = 9) recorded at either 298 or 50 K was of satisfactory quality up to 10.5 $Å^{-1}$ [Fig. 1(a)]. A reasonable fit to the room temperature data was achieved with 8.9 oxygen atoms at 2.33 Å, presumably comprising hydration water molecules and probably also framework oxygens (fit A in Table 1). These values are very similar to those obtained from a recent XAS study of the hydration structure of yttrium(III) cations in liquid and glassy states.[23] A parallel result was obtained by Berry *et al.* for Eu^{3+}-exchanged zeolite-Y, for which EXAFS investigations showed the hydration structure of the exchanged rare earth ion to be similar to that found in aqueous Eu^{3+} solutions.[24] The large Debye–Waller factor ($2\sigma^2$) obtained for the erbium–oxygen shell (0.03 $Å^2$) indicates substantial thermal and/or static disorder. Cooling the sample to 50 K did not change the refined Er–O distance but the final fitted co-ordination number was slightly lower. The Debye–Waller factor only decreased to 0.02 $Å^2$, which points to a considerable dispersion in the Er–O distances.

The theoretical fits to both the room temperature and low temperature Er L_{III}-edge EXAFS of Er^{3+}-doped ETS-10 (Ti/Er = 9) were substantially improved by the inclusion of a shell for 1.25–1.5 titanium atoms at 3.30–3.32 Å, which resulted in a 35–40% decrease in the fit index [fit B in Table 1, Fig. 1(a)]. This result is in line with previous expectations that the exchanged Er^{3+} ions reside close to the (negatively charged) TiO_6 octahedra.[7] The existence of this shell suggests that some Er^{3+} is partially bonded to framework oxygen atoms. Analogous results were reported previously in some Er^{3+}- and Eu^{3+}-exchanged Y-zeolites,[24,25] and Eu^{3+}-exchanged zeolite-A.[14] The single crystal X-ray structure of Na–ETS-10 was recently reported and it was found that the sodium cations occupy two nonequivalent positions within the 7-ring cages and in the 12-ring channels.[20] One sodium has two titanium atom neighbours at 3.15 Å while the other has two titanium atoms at 3.20 Å. The EXAFS-derived Er···Ti distance of 3.3 Å in Er^{3+}-doped ETS-10 therefore seems plausible.

The Er L_{III}-edge EXAFS of Er^{3+}-doped ETS-10 (Ti/Er = 23) recorded at either 298 or 50 K was of satisfactory quality up to 8.8 $Å^{-1}$. Analysis of the first co-ordination shell for oxygen gave very similar results to those obtained for the sample with the higher erbium loading (Table 1). Only for the low temperature data was it possible to fit an additional shell of 1.25 Ti atoms at 3.33 Å. X-Ray absorption spectra were also recorded at 298 and 50 K for this sample calcined to 973 K. In

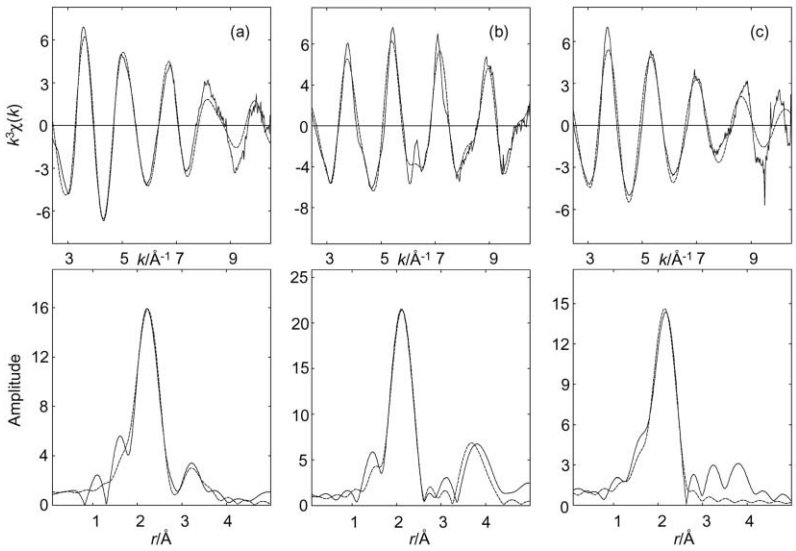

Fig. 1 Er L_{III}-edge k^3-weighted transmission EXAFS spectra recorded at 50 K and Fourier transforms, phase-shift corrected for oxygen (——, experimental; – – – – –, curved wave theory), of (a) Er^{3+}-doped ETS-10 (Ti/Er = 9) (fit B), (b) Er^{3+}-doped narsarsukite (Ti/Er = 9) (fit B) and (c) Er^{3+}-doped glassy (Ti/Er = 9) (fit A).

Table 1 Structural parameters obtained from erbium L_{III}-edge EXAFS data recorded at 298 or 50 K for Er^{3+}-doped ETS-10 samples

Sample	T/K[a]	S[b]	Fit	A[c]	CN[d]	r/Å[e]	$2\sigma^2$/Å^{2}[f]	EF/eV[g]	R (%)
Er^{3+}-Doped ETS-10 (Ti/Er = 9)	298	2	A	O	8.9(2)	2.331(5)	0.0296(10)	−7.9(3)	23.4
			B	O	8.9(2)	2.330(4)	0.0294(8)	−7.8(3)	16.7
				Ti	1.5(2)	3.303(10)	0.0235(28)		
Er^{3+}-Doped ETS-10 (Ti/Er = 9)	50	1	A	O	8.2(2)	2.330(5)	0.0212(10)	−7.9(4)	25.6
			B	O	8.2(2)	2.331(4)	0.0211(8)	−8.0(3)	20.3
				Ti	1.25(20)	3.318(11)	0.0149(26)		
Er^{3+}-Doped ETS-10 (Ti/Er = 23)	298	2	A	O	8.9(3)	2.333(8)	0.0309(16)	−7.5(5)	30.8
Er^{3+}-Doped ETS-10 (Ti/Er = 23)	50	2	A	O	8.7(3)	2.344(6)	0.0254(13)	−8.0(5)	26.0
			B	O	8.7(3)	2.340(5)	0.0251(11)	−7.8(4)	21.7
				Ti	1.25(21)	3.326(13)	0.0126(35)		

[a]T = measurement temperature. [b]S = number of averaged spectra. [c]A = atom type. [d]CN = co-ordination number. [e]r = inter-atomic distance. Standard deviations are given in parentheses. The real errors in EXAFS-derived co-ordination numbers and distances for well-defined shells are estimated to be 20 and 1.5% respectively. [f]Debye–Waller factor; σ = root-mean-square deviation of inter-atomic distance about r. [g]EF = edge position (fermi energy), relative to calculated vacuum zero.

both cases analysis of the first shell gave 6.8 oxygens at 2.27 Å (Table 2). No acceptable improvement in the theoretical fits could be achieved by the inclusion of additional shells.

Er^{3+}-Doped narsarsukite (Ti/Er = 9), formed by calcination of Er^{3+}-doped ETS-10 at 1073 K, provided markedly different EXAFS and Fourier transform (FT) compared to those obtained for the ion-exchanged sample calcined at 973 K [Fig. 1(b)]. Two peaks are evident in the FT corresponding to backscattering atoms in the first and second co-ordination spheres. Analysis of the first shell gave a clear minimum in the fit index with 6 oxygen atoms at 2.20 Å ($2\sigma^2$ = 0.008 Å^2, fit A in Table 2). The goodness of fit R was subsequently improved from 37.7 to 22.6% by fitting 5 silicon atoms at 3.78 Å ($2\sigma^2$ = 0.009 Å^2, fit B). The Er···Si distance seems reasonable for Er–O–Si bonding, although it would require a long Si–O distance and/or a large Si–O–Er angle. There was no evidence for Er···Er correlations within the short range order, in particular no shell at 3.5 Å which would be characteristic of Er_2O_3-like

Table 2 Structural parameters obtained from erbium L_{III}-edge EXAFS data recorded at 298 or 50 K for calcined Er^{3+}-doped ETS-10 samples

Sample	CT/K[a]	T/K	S	Fit	A	CN	r/Å	$2\sigma^2$/Å^2	EF/eV	R (%)
Er^{3+}-Doped ETS-10 (Ti/Er=23)	973	298	2	A	O	6.8(3)	2.273(8)	0.0214(16)	−8.8(7)	30.0
Er^{3+}-Doped ETS-10 (Ti/Er = 23)	973	50	1	A	O	6.8(3)	2.270(8)	0.0152(14)	−8.6(7)	29.5
Er^{3+}-Doped narsarsukite (Ti/Er = 9)	1073	50	1	A	O	6.0(3)	2.194(6)	0.0086(10)	−7.1(7)	37.7
				B	O	6.0(2)	2.196(4)	0.0082(7)	−7.7(4)	22.6
					Si	5.0(5)	3.777(7)	0.0094(16)		
Er^{3+}-Doped narsarsukite (Ti/Er = 23)	1073	50	2	A	O	6.0(4)	2.172(9)	0.0073(17)	−6.6(10)	38.3
				B	O	6.0(3)	2.173(7)	0.0068(14)	−6.9(8)	32.2
					Si	5.0(9)	3.732(18)	0.0127(45)		
Er^{3+}-Doped glassy (Ti/Er = 9)	1473	298	2	A	O	6.0(3)	2.241(7)	0.0197(13)	−7.6(6)	32.8
Er^{3+}-Doped glassy (Ti/Er = 9)	1473	50	1	A	O	6.3(2)	2.244(6)	0.0171(10)	−7.7(5)	27.6
Er^{3+}-Doped glassy (Ti/Er = 23)	1473	50	2	A	O	7.0(2)	2.239(6)	0.0160(11)	−6.8(5)	24.4

[a]CT = calcination temperature to which Er^{3+}-doped ETS10 was submitted.

environments.[26] The average Er–O bond length is significantly shorter than that for Er_2O_3 (6 oxygens at 2.26 Å,[26] $2\sigma^2$ = 0.012 Å^2). Furthermore, the low Debye–Waller factor for this shell indicates a small dispersion of distances, implying that one family of erbium sites dominates. Analogous species have been identified previously in erbium-doped amorphous silicon co-doped with oxygen (*a*-SiO_x:H).[27] In another EXAFS study, erbium in aluminosilicate glass was found to have 6.4 nearest oxygen neighbours at a distance of 2.22 Å, but with a much larger Debye–Waller factor of 0.031 Å^2.[15] The problem of Er clustering in silica–titania–alumina glasses has been studied recently by Almeida and co-workers.[28,29]

The exact location of the ErO_6 units within the host structure is of considerable interest. Previous photoluminescence and solid state ^{29}Si MAS NMR studies provided good evidence that the erbium ions are located in the narsarsukite phase.[7] In the natural mineral narsarsukite, sodium cations are located in small cavities. There are seven nearest oxygen neighbours at distances between 2.39 and 2.72 Å, two silicon atoms at 3.2 Å and two titanium atoms at 3.23 Å. It therefore seems unlikely that in erbium-doped narsarsukite Er^{3+} ions are located predominantly in the cavity positions normally occupied by sodium ions. Another possibility that must be considered is that erbium ions substitute for titanium atoms in the narsarsukite framework. Partial substitutions of Zr^{4+}, Fe^{3+}, Al^{3+} and Mn^{2+} for the Ti in narsarsukite have been reported.[30] It is also known that erbium ions can substitute onto the titanium sites of various framework oxides, for example rubidium titanyl arsenate.[31] In the mineral narsarsukite, [TiO_6] octahedra share corners to form infinite chains. The octahedra are distorted, with one short (1.90 Å) and one long (2.07 Å) Ti–O distance in the Ti–O–Ti linkage, and 4 Ti–O distances at 1.97 Å. In the second co-ordination sphere, four Si are at 3.33 Å, one Ti at 3.81 and one Ti at 4.14 Å. Careful analysis of the Er L_{III}-edge EXAFS of Er^{3+}-doped narsarsukite validated the existence of a shell for Ti atoms at about 4 Å. Thus, a reasonable fit was obtained with six oxygens at 2.19 Å and two titaniums at 3.99 Å (R = 27.5%).[32] However, the Debye–Waller factor was low (0.003 Å^2) with a large statistical error (70%). The statistics were improved by increasing the number of titanium atoms in the second shell to 6.[33] Inclusion of shells for both silicon and titanium produced the best fit to the data (R = 21.0%) but, again, the statistical errors were unacceptably large.[34] Future Ti K-edge EXAFS studies may confirm the existence of a Ti···Er correlation at 4 Å.

The EXAFS of Er^{3+}-doped narsarsukite with the lower erbium loading (Ti/Er = 23) was analysed up to 8.8 Å^{-1}. Despite the poorer data quality (which gave rise to larger statistical errors), it was evident from the curve-fitting results that the average local environment of erbium ions in the sample is similar to that seen in the sample with the higher loading (Table 2). The main difference is that the final fitted Er–O and Er···Si distances were slightly shorter (2.17 and 3.73 Å respectively). The glassy erbium-doped samples, formed by calcination of Er^{3+}-doped ETS-10 at 1473 K, provided different EXAFS spectra again and erbium was found to have between 6 and 7 nearest oxygen neighbours at 2.24 Å ($2\sigma^2$ = 0.017 Å^2) but no well-defined second nearest neighbour shell could be identified [Fig. 1(c)]. Comparison of the Debye–Waller factors with those found for Er-doped narsarsukite indicates a larger dispersion in Er–O distances, consistent with the amorphous nature of the samples.

Raman spectroscopy

Raman spectra of narsarsukite and Er^{3+}-doped narsarsukite with different amounts of erbium are shown in Fig. 2. The Raman spectrum of narsarsukite is dominated by a peak at *ca.* 775 cm^{-1} attributed to Ti–O stretching-type vibrations of the TiO_6 units.[35] Doped samples display anatase peaks at 144, 200 and 399 (O–Ti–O bending-type vibrations) and at 639 cm^{-1} (Ti–O bond stretching-type vibrations).[36] Another peak at *ca.* 125 cm^{-1} is attributed to a surface phonon mode of anatase nanocrystals in the narsarsukite matrix.[37] The presence of very small ($\leq$10 nm) anatase crystallites is indicated by the ratio between the intensities of the surface phonon (at *ca.* 125 cm^{-1}) and the main anatase peak (*ca.* 144 cm^{-1}).[37] It should be stressed that no anatase XRD reflections are observed for both narsarsukite and Er^{3+}-doped narsarsukite samples (see Figs. 2 and 4 in ref. 7). The full-width at half-maximum (FWHM) of the main peak at 775 cm^{-1} increases by *ca.* 20 cm^{-1} from that of the undoped narsarsukite sample (with Ti/Er = ∞) to the doped sample (with Ti/Er = 9). The increasing FWHM of the 775 cm^{-1} peak and the increasing intensity of the anatase peaks as the erbium content increases both suggest the isomorphous substitution of Ti^{4+} for Er^{3+} in the narsarsukite framework. Indeed, the framework isomorphous substitution in titanosilicates such as ETS-10 is sometimes accompanied by a broadening and slight shift of the 775 cm^{-1} Raman band.[38] On the other hand, upon erbium insertion the expelled titanium is segregated as a TiO_2-rich phase and subsequently crystallises as anatase.

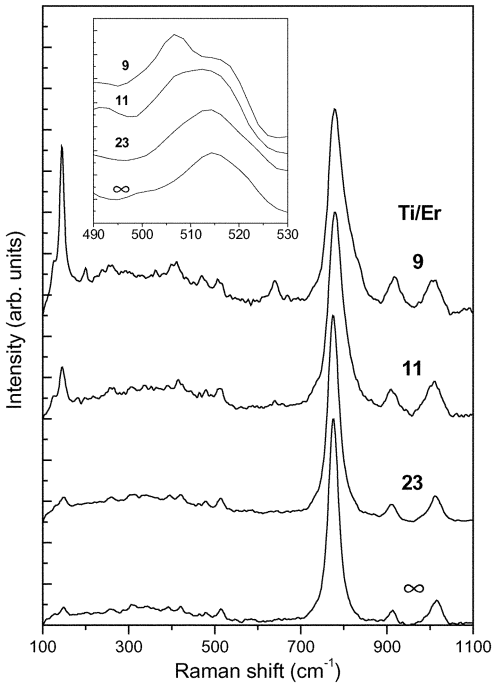

Fig. 2 Raman spectra (λ_{exc} = 1064 nm) of Er^{3+}-doped narsarsukite. The Ti/Er molar ratios are indicated.

The inset in Fig. 2, shows that as the Er^{3+} content increases the band at *ca.* 515 cm^{-1} firstly broadens and subsequently a new band appears at *ca.* 507 cm^{-1}. We note that a Raman band at 490–530 cm^{-1} (also infrared-active, not shown) is present in all undoped ETS-10 and ETS-10 calcined materials (not shown) and is ascribed to O–Ti–O and Ti–O–Ti bond bending type vibrations.[39]

Photoluminescence spectroscopy

Fig. 3 shows the excitation spectra of Er^{3+}-doped titanosilicates, recorded at 14 and 300 K. The sharp lines are assigned to intra-4f^{11} transitions between the $^4I_{15/2}$ and the $^4F_{9/2,\ 7/2,\ 5/2,\ 3/2}$, $^4S_{3/2}$, $^2H_{11/2,\ 9/2}$, $^4G_{11/2}$, and $^2K_{15/2}$ levels, and the sidebands observed in the lower energy regions of the $^4I_{15/2} \rightarrow {}^2H_{11/2}$ and $^4I_{15/2} \rightarrow {}^4G_{11/2}$ transitions (ΔJ = 2) are associated with phonon-assisted anti-Stokes vibronic components.[7] Er^{3+}-Doped narsarsukite gives an additional vibronic sideband, already reported in a previous work,[7] seen on the lower energy side of the $^4I_{15/2} \rightarrow {}^4F_{7/2}$ transition. The presence of

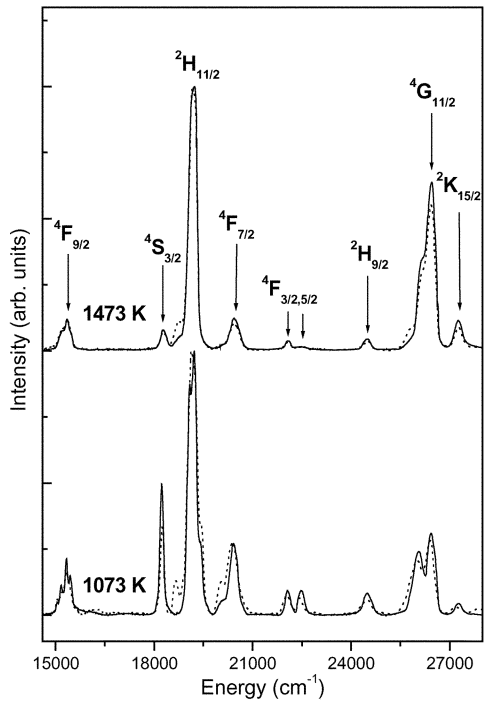

Fig. 3 Excitation spectrum (λ_{em} = 1542 nm) of Er^{3+}-doped titanosilicates (Ti/Er = 23) calcined at 1073 K (synthetic narsarsukite) and 1473 K (glassy phase), recorded at 14 (solid line) and 300 K (dotted line).

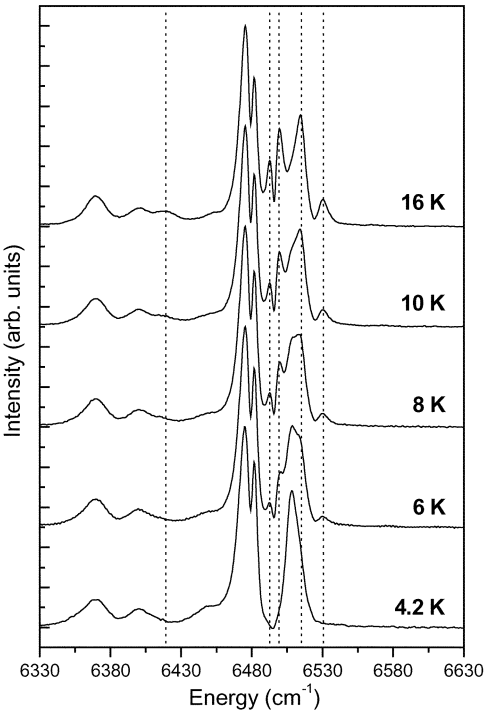

Fig. 4 Infrared emission spectra (λ_{exc} = 488 nm) of Er^{3+}-doped narsarsukite (Ti/Er = 23) recorded between 4.2 and 16 K. The dashed guides indicate electronic lines present at 4.2 K but enhanced with temperature.

this sideband (ΔJ = 4) violates the selection rule that arises from the theoretical approaches to vibronic line intensity of lanthanide ions.[40–43] Similar violations, generally associated with inactive infrared vibrational modes, have been observed for Pr^{3+} ($^3H_4 \rightarrow {}^3P_0$),[40,44] Eu^{3+} ($^7F_0 \rightarrow {}^5D_4$),[43] and Tm^{3+} ($^1D_2 \rightarrow {}^3H_6$).[41,42]

The phonon energy corresponding to the observed sidebands is estimated by the energy difference relative to the corresponding electronic transitions. The values obtained for the two vibronic lines associated with the $^4I_{15/2} \rightarrow {}^2H_{11/2}$ and $^4I_{15/2} \rightarrow {}^4G_{11/2}$ transitions are similar, *ca.* 450–530 cm^{-1} and no significant variation with the calcination temperature could be detected. This phonon frequency may be associated with the Raman- and infrared-active mode detected at *ca.* 500 cm^{-1} in Fig. 2. The phonon energy associated with the $^4I_{15/2} \rightarrow {}^4F_{7/2}$ vibronic sideband is lower, *ca.* 330 cm^{-1}. This value is similar to the values found for other lanthanide-based materials[45–49] and probably corresponds to Er–O local vibrational modes, inactive in the Raman and infrared.[50] The electron–phonon coupling parameter, g, which is a relative measure of the phonon sideband line strength, may be evaluated by calculating the intensity ratio between the vibronic and the associated electronic lines.[45–49] In order to prevent the saturation of the $^4I_{15/2} \rightarrow {}^2H_{11/2}$, $^4F_{7/2}$, $^4G_{11/2}$ electronic transitions, g was determined for Er^{3+}-doped titanosilicates with low Er^{3+} concentration (Ti/Er = 23). The value obtained for the vibronic sidebands associated with both $^4I_{15/2} \rightarrow {}^2H_{11/2}$ and $^4I_{15/2} \rightarrow {}^4G_{11/2}$ electronic lines is *ca.* 0.1. There is no appreciable variation in g with the calcination temperature. However, the value found for the vibronic transition associated with the $^4I_{15/2} \rightarrow {}^4F_{7/2}$ line (which is, as stated above, characteristic of Er^{3+}-doped narsarsukite) is approximately twice this value, at *ca.* 0.2.

The photoluminescence features of Er^{3+}-doped titanosilicates have been reported recently.[7] No emission is observed for hydrated Er^{3+}-doped ETS-10. The Er^{3+} ions are optically active only for samples calcined at temperatures above *ca.* 973 K. The 14 K infrared emission spectrum of Er^{3+}-doped narsarsukite displays a $^4I_{13/2} \rightarrow {}^4I_{15/2}$ local-field Stark structure of *ca.* 14 distinct lines (see Fig. 10 in ref. 7), suggesting the presence of, at least, two different local Er^{3+} environments. The possibility that some of these lines result from next-lowest excited levels of the J = 13/2 multiplet (the so-called satellite or "hot" photoluminescence lines[51]) must be considered and, hence, luminescence measurements have been carried out at low temperature. More Stark components are observed at 4.2 K (and more clearly at 6 K, Fig. 4) than are expected for Er^{3+} centres in cubic or lower than cubic symmetry (five and eight lines, respectively), confirming the presence of more than one optically-active Er^{3+} local environment.

Fig. 5 shows the infrared emission spectra of Er^{3+}-doped narsarsukite recorded over the range 4.2 to 300 K. Up to 30 K, no satellite photoluminescence lines could be detected in the infrared emission spectra of Er^{3+}-doped narsarsukite. However, at 50 K two hot lines (termed HL_1 and HL_2), could be detected, shifted *ca.* 64 cm^{-1} (towards higher energies) from the lowest excited crystal-field-split level of the $^4I_{13/2}$ multiplet. A third line (HL_3), originating from the same excited level, is seen at 100 K. The characteristic temperature dependence of both the electronic and satellite lines confirms this assignment.[51] The photoluminescence intensity ratio $I_{HL}/(I_{ET} + I_{HL})$ (where I_{ET} and I_{HL} are the intensities of the electronic and satellite lines, respectively) increases with increasing temperature with an activation energy equal to the energy difference between the electronic and satellite lines (*ca.* 64 cm^{-1}).

Lifetime measurements of the $^4I_{13/2}$ excited state (*ca.* 1.54 μm) have been performed on the Er^{3+}-doped titanosilicates calcined at temperatures between 973 and 1473 K (not shown). The frequency dependency of the phase-angle shift is essentially linear, corresponding to $^4I_{13/2}$ lifetimes of 5.4 ± 0.1 (sample calcined at 973 K), 7.8 ± 0.2 (Er^{3+}-doped narsarsukite), and 9.9 ± 0.3 ms (Er^{3+}-doped glass). The values found for the titanosilicate calcined at 1223 K and Er^{3+}-doped narsarsukite are identical and of the order of magnitude of the lifetimes reported for other related materials, such as aluminosilicates

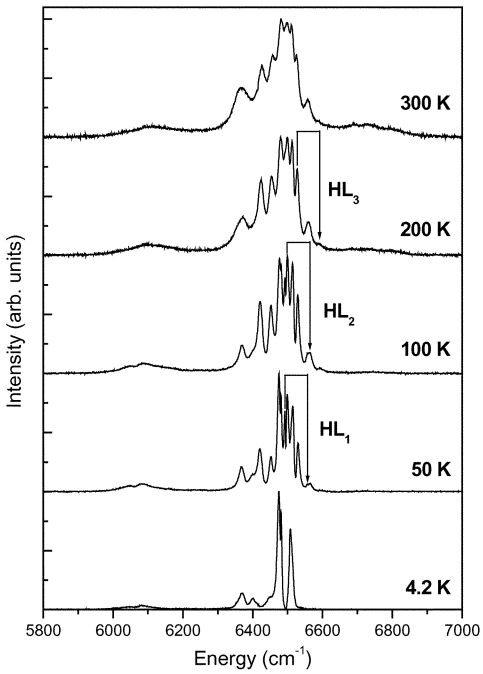

Fig. 5 Infrared emission spectra (λ_{exc} = 488 nm) of Er^{3+}-doped narsarsukite (Ti/Er = 23) recorded between 4.2 and 300 K. The arrows depict the positions of the satellite lines.

(3.5 ms),[52] titanosilicates (6.4 ms),[53] borosilicates (9.9 ms),[51] phosphosilicates (12 ms),[1] and sodium silicates (20 ms).[53]

Conclusions

Er L_{III}-edge EXAFS studies of Er^{3+}-doped ETS-10 support the view that the exchanged Er^{3+} ions reside close to the (negatively charged) TiO_6 octahedra.[7] In ETS-10, Er^{3+} is partially bonded to framework oxygen atoms and hydration water molecules and this is in line with results reported for some Er^{3+} and Eu^{3+}-exchanged Y-zeolites,[24,25] and Eu^{3+}-exchanged zeolite-A.[14] The EXAFS-derived Er···Ti distance (3.3 Å) is similar to the Na···Ti distances (3.15–3.20 Å) reported previously for Na-ETS-10.[20] The exact location of the ErO_6 units within the host structure of Er^{3+}-doped narsarsukite, formed by calcination of Er^{3+}-doped ETS-10 at 1073 K, is still an open question. However, it is unlikely that the Er^{3+} ions are located predominantly in the cavity positions normally occupied by Na^+ ions and, most likely, they substitute for Ti^{4+} ions in the narsarsukite framework. Another important conclusion derived from EXAFS data for all of the samples studied is that there is no evidence for Er···Er correlations within the short range order and, therefore, no significant clustering of erbium atoms occurs.

Raman spectroscopy provides further evidence for the insertion of Er^{3+} ions in the framework of narsarsukite. This is indicated by the increasing FWHM of the 775 cm^{-1} peak and the increasing intensity of the anatase peaks as the erbium content increases. In addition, as the Er^{3+} content increases a band at *ca.* 515 cm^{-1} firstly broadens and subsequently a new peak appears at *ca.* 507 cm^{-1}.

The number of lines in the infrared emission spectrum of synthetic narsarsukite indicates the presence of two optically-active erbium centres with very similar local environments and an average $^4I_{13/2}$ lifetime of 7.8 ms. The excitation spectra of Er^{3+}-doped narsarsukite exhibit a phonon-assisted anti-Stokes sideband which corresponds to a local vibrational frequency of *ca.* 330 cm^{-1}, with high electron–phonon coupling, *ca.* 0.2. Since this band is associated with Er–O vibrations and EXAFS data show that no clustering of erbium ions occurs, this is additional evidence for framework Er^{3+} insertion.

Acknowledgement

We thank ESRF for the provision of facilities and also Michael Borowski, Station BM29, for his help and technical assistance. We also wish to thank J. Soares and C. Azevedo for assistance with the FTIR and Raman measurements and FCT, PRAXIS XXI, POCTI, FEDER for financial support.

References

1 A. Polman, *J. Appl. Phys.*, 1997, **82**, 1.
2 G. Dieke, *Spectra and Energy Levels of Rare Earth Ions in Crystals*, John Wiley & Sons, New York, 1965.
3 E. Desurvire, R. J. Simpson and P. C. Becker, *Opt. Lett.*, 1987, **12**, 888.
4 M. W. Anderson, O. Terasaki, T. Ohsuna, A. Philippou, S. P. MacKay, A. Ferreira, J. Rocha and S. Lidin, *Nature*, 1994, **367**, 347.
5 J. Rocha and M. W. Anderson, *Eur. J. Inorg. Chem.*, 2000, 801.
6 Y. A. Pyatenko and Z. V. Pudovkina, *Kristallografiya*, 1960, **5**, 563.
7 J. Rocha, L. D. Carlos, J. P. Rainho, Z. Lin, P. Ferreira and R. M. Almeida, *J. Mater. Chem.*, 2000, **10**, 1371.
8 J. P. Rainho, L. D. Carlos and J. Rocha, *J. Lumin.*, 2000, **87–89**, 1083.
9 G. Vlaic, D. Andreatta and P. E. Colavita, *Catal. Today*, 1998, **41**, 261.
10 S. Taboada, A. de Andres, J. E. Munoz-Santiuste, C. Prieto, J. L. Martinez and A. Criado, *Phys. Rev. B*, 1994, **50**, 9157.
11 L. D. Carlos, R. A. S. Ferreira, V. D. Z. Bermudez, C. Molina, L. A. Bueno and S. J. L. Ribeiro, *Phys. Rev. B*, 1999, **60**, 10042.
12 P. M. Peters and S. N. Houde-Walter, *J. Non-Cryst. Solids*, 1998, **239**, 162.
13 M. A. Marcus and A. Polman, *J. Non-Cryst. Solids*, 1991, **136**, 260.
14 S. L. Suib, R. P. Zerger, G. D. Stucky, T. I. Morrison and G. K. Shenoy, *J. Chem. Phys.*, 1984, **80**, 2203.
15 P. M. Peters and S. N. Houde-Walter, *Appl. Phys. Lett.*, 1997, **70**, 541.
16 N. Binsted, EXCURV98: CCLRC Daresbury Laboratory computer program, 1998.
17 S. J. Gurman, N. Binsted and I. Ross, *J. Phys. C*, 1984, **17**, 143.
18 R. W. Joyner, K. J. Martin and P. Meehan, *J. Phys. C*, 1987, **20**, 4005.
19 B. Rupp, B. Smith and J. Wong, *Comput. Phys. Commun.*, 1992, **67**, 543.
20 X. Wang and A. J. Jacobson, *Chem. Commun.*, 1999, 973.
21 D. R. Peacor and M. J. Buerger, *Am. Mineral.*, 1962, **47**, 539.
22 J. R. Lakowicz, *Principles of Fluorescence Spectroscopy*, Kluwer Academic Plenum Publishers, New York, 2nd edn., 1999.
23 The structural chemistry of Y^{3+} is pertinent to that of Er^{3+} since the two ions have similar ionic radii when in 8-fold co-ordination (1.02 and 1.00 Å respectively). See: S. Díaz-Moreno, A. Muñoz-Páez and J. Chaboy, *J. Phys. Chem. A*, 2000, **104**, 1278.
24 F. J. Berry, M. Carbucicchio, A. Chiari, C. Johnson, E. A. Moore, M. Mortimer and F. F. F. Vetel, *J. Mater. Chem.*, 2000, **10**, 2131.
25 F. J. Berry, J. F. Marco and A. T. Steel, *J. Alloys Compd.*, 1993, **194**, 167.
26 EXAFS-Derived structural parameters for Er_2O_3 at 50 K (co-ordination numbers and crystal structure distances given in parentheses): Er–O = 2.259(6) Å, $2\sigma^2$ = 0.0110(11) $Å^2$ (N = 6, r_{cryst} = 2.27 Å); Er···Er = 3.508(2) Å, $2\sigma^2$ = 0.0049(2) $Å^2$ (N = 6, r_{cryst} = 3.49 Å); Er···Er = 3.985(2) Å, $2\sigma^2$ = 0.0060(3) $Å^2$ (N = 6, r_{cryst} = 4.00 Å); Er···Er = 5.279(6) Å, $2\sigma^2$ = 0.0081(9) $Å^2$ (N = 6, r_{cryst} = 5.30 Å); Er···Er = 6.069(14) Å, $2\sigma^2$ = 0.0040(24) $Å^2$ (N = 3, r_{cryst} = 6.02 Å); Er···Er = 6.310(20) Å, $2\sigma^2$ = 0.0121(41) $Å^2$ (N = 9, r_{cryst} = 6.32 Å); Er···Er = 6.643(8) Å, $2\sigma^2$ = 0.0061(11) $Å^2$ (N = 9, r_{cryst} = 6.62 Å); EF = −8.9(5) eV, R = 20.8%, Δk = 2.2–14.8 $Å^{-1}$.
27 C. Piamonteze, A. C. Iñiguez, L. R. Tessler, M. C. Martins Alves and H. Tolentino, *Phys. Rev. Lett.*, 1998, **81**, 4652.
28 F. D'Acapito, S. Mobilio, L. Santos and R. M. Almeida, *Appl. Phys. Lett.*, 2001, **78**, 2676.
29 F. D'Acapito, S. Mobilio, P. Gastaldo, D. Barbier, L. F. Santos, O. Martins and R. M. Almeida, *J. Non-Cryst. Solids*, in the press.
30 C. Wagner, G. C. Parodi, M. Semet, J. L. Robert, M. Berrahma and D. Velde, *Eur. J. Mineral.*, 1991, **3**, 575.
31 M. T. Anderson, M. L. F. Phillips, M. B. Sinclair and G. D. Stucky, *Chem. Mater.*, 1996, **8**, 248.

32 Er–O = 2.190(5) Å, $2\sigma^2$ = 0.0081(8) Å^2 (N = 6); Er···Ti = 3.995(9) Å, $2\sigma^2$ = 0.0029(20) Å^2 (N = 2); EF = −6.6(5) eV, R = 27.5%, Δk = 2.5–10.5 Å^{-1}.
33 Er–O = 2.188(4) Å, $2\sigma^2$ = 0.0083(7) Å^2 (N = 6); Er···Ti = 4.016(9) Å, $2\sigma^2$ = 0.0188(21) Å^2 (N = 6); EF = −6.4(5) eV, R = 27.1%, Δk = 2.5–10.5 Å^{-1}.
34 Er–O = 2.194(4) Å, $2\sigma^2$ = 0.0083(6) Å^2 (N = 6); Er···Ti = 4.055(28) Å, $2\sigma^2$ = 0.0177(67) Å^2 (N = 2); Er···Si = 3.766(11) Å, $2\sigma^2$ = 0.0082(22) Å^2 (N = 4); EF = −7.4(4) eV, R = 20.9%, Δk = 2.5–10.5 Å^{-1}.
35 Y. Su, M. L. Balmer and B. C. Bunker, *J. Phys. Chem. B*, 2000, **104**, 8160.
36 T. Ohsaka, F. Izumi and Y. Fujiki, *J. Raman Spectrosc.*, 1978, **7**, 321.
37 J. P. Rainho, J. Rocha, L. D. Carlos and R. M. Almeida, *J. Mater. Res.*, 2001, **16**, 2369.
38 Z. Lin, J. Rocha, A. Ferreira and M. W. Anderson, *Colloids Surf., A*, 2001, **179**, 133.
39 B. Mihailova, V. Valtchev, S. Mintova and L. Konstantinov, *Zeolites*, 1996, **16**, 22.
40 O. L. Malta, *J. Phys. Chem. Solids*, 1995, **56**, 1053.
41 A. F. Campos, C. de Melo Donegá and O. L. Malta, *J. Lumin.*, 1997, **72–74**, 166.
42 A. F. Campos, A. Meijerink, C. de Melo Donegá and O. L. Malta, *J. Phys. Chem. Solids*, 2000, **61**, 1489.
43 C. de Melo Donegá, A. Meijerink and G. Blasse, *J. Phys. Condens. Matter.*, 1992, **4**, 8889.
44 M. Tanaka and T. Kushida, *Phys. Rev. B*, 1999, **60**, 14732.
45 S. Todoroki, K. Hirao and N. Soga, *J. Non-Cryst. Solids*, 1992, **143**, 46.
46 K. Soga, H. Inoue and A. Makishima, *J. Lumin.*, 1993, **55**, 17.
47 M. Dejneka, E. Snitzer and R. E. Riman, *J. Lumin.*, 1995, **65**, 227.
48 S. Tanabe, S. Todoroki, K. Hirao and N. Soga, *J. Non-Cryst. Solids*, 1990, **122**, 59.
49 S. J. L. Ribeiro, R. E. O. Diniz, Y. Messaddeq, L. A. Nunes and M. A. Aegerter, *Chem. Phys. Lett.*, 1994, **220**, 214.
50 G. Blasse, in *Advances in Non-Radiative Processes in Solids*, ed. B. Di Bartolo, Plenum Press, NY, 1991, p. 287.
51 H. H. Przybylinska, W. Jantsch, Y. Suprun-Belevitch, M. Stepikhova, L. Palmetshofer, G. Hendorfer, A. Kozanecki, R. J. Wilson and B. J. Sealy, *Phys. Rev. B*, 1996, **54**, 2532.
52 M. Benatsou, B. Capoen, M. Bouazaoui, W. Tchana and J. P. Vilcot, *Appl. Phys. Lett.*, 1997, **71**, 428.
53 X. Orignac, D. Barbier, X. M. Du, R. M. Almeida, O. McCarthy and E. Yeatman, *Opt. Mater.*, 1999, **12**, 1.